

Fatigue Crack Growth Resistance of Nanocrystalline Copper

R.K. Rajgarhia¹, A. Saxena¹, C. Jackson²

University of Arkansas, Fayetteville, Arkansas, USA; ²Arkansas Tech University, Russellville, AR

Abstract

Fatigue crack growth behavior of nanocrystalline copper with grain size less than 250 nm is studied and compared to its microcrystalline counterpart. The nanocrystalline samples are prepared by processing commercially pure Cu using the equal channel angular extrusion (ECAE) process. The microcrystalline samples are prepared from the same Cu material and normalized at 500 °C for 2.5 hours. All samples are tested as per the ASTM E647 standard at room temperature under tension-tension loading, and data over a wide range of stress intensity levels is presented. A cross-over in the behavior of two materials has been observed showing that the nanocrystalline copper has a higher fatigue crack growth resistance over the middle Paris regime, but a lower fatigue crack growth resistance in the near threshold regime. To explain the cross-over behavior, fractography and microhardness measurements in the plastic zone are conducted. These results show evidence of softening due to grain coalescence and growth in recovery and grain coalescence in the plastic zone for nanocrystalline Cu and work hardening for microcrystalline Cu. The formation of oxide particles on the fracture surface in the threshold region of microcrystalline Cu are observed that cause crack closure, resulting in a lower effective ΔK (ΔK_{eff}).

1. Introduction

It is well known that the mechanical properties of crystalline materials can be significantly influenced by controlling the grain size. Crystalline materials with grain size less than 100nm, also known as nanocrystalline materials, have exhibited multi-fold increase in mechanical strength compared to their microcrystalline counterparts [1, 2]. This dependence of grain size on the mechanical strength was first described by the Hall-Petch relationship according to which the yield strength is inversely proportional to the square-root of the grain size [3, 4]. These unique properties are attributed to the large volume fraction of grain boundaries that restrict Frank-Reed type dislocation mechanisms observed in coarse grained materials and increase pileups of dislocations emitted from grain boundaries, thereby causing increase in the mechanical strength [5, 6]. Although the improvement in the mechanical strength of nanocrystalline materials is well accepted, there is limited information available about the fatigue performance of these materials. Since most failures involve fatigue loading, it is important to evaluate the fatigue resistance of nanocrystalline materials before using them for structural applications.

In a previous study by our research group, it has been shown that nanocrystalline Cu processed using ECAE has superior high cycle fatigue strength compared to microcrystalline Cu [7, 8]. This increase in strength indicates a higher resistance

to crack initiation in nominally smooth specimens. In this work, comparison of fatigue crack growth resistance of nanocrystalline Cu is presented, and compared with microcrystalline Cu.

2. Material preparation

The material selected for this work is commercially pure Cu (99.95%), OFHC CDA102. The material was purchased in a bar stock of 25.4 mm x 25.4 mm square cross section, in microcrystalline form. This material has high electrical conductivity (101% International Annealed Copper Standard, IACS) and is typically used for electrical conductors. To refine the grain size, the material is processed using the ECAE process [9], route 4-E at room temperature. The net strain (ε_N) in the material during ECAE process can be calculated as per Eq. 1 [9]. In Eq. 1, N is the number of extrusion passes, ψ and ϕ are the interior angles of the die. For the ECAE process used in this work, $N = 4$, $\psi = \phi = 90^\circ$ and the net strain is calculated to be 363%. The ECAE process is the only nanocrystalline material processing technique with the ability to produce fully-dense, bulk materials with ultrafine grain size, and in large enough quantities to machine specimens that comply with the ASTM standards. For comparison studies, the as-purchased material is annealed at 500 °C for 2 hours to completely normalize the material and ensure that the microstructure is in microcrystalline form.

$$\varepsilon_N = \frac{N}{\sqrt{3}} \left[2 \cot \left(\frac{\phi + \psi}{2} \right) + \psi \right] \quad \text{Eq. (1).}$$

The grain size measurements are conducted using TEM and SEM (back scatter imaging) on samples prepared by electropolishing. The results from the TEM analysis are shown in Fig. 1. The average grain size is about 350.74 nm for nanocrystalline Cu and 2.05 μm for microcrystalline Cu and is calculated using Abrams three circle method as per ASTM E112. Similar grain size results are obtained from the SEM analysis. Although ECAE processed Cu is not ‘truly’

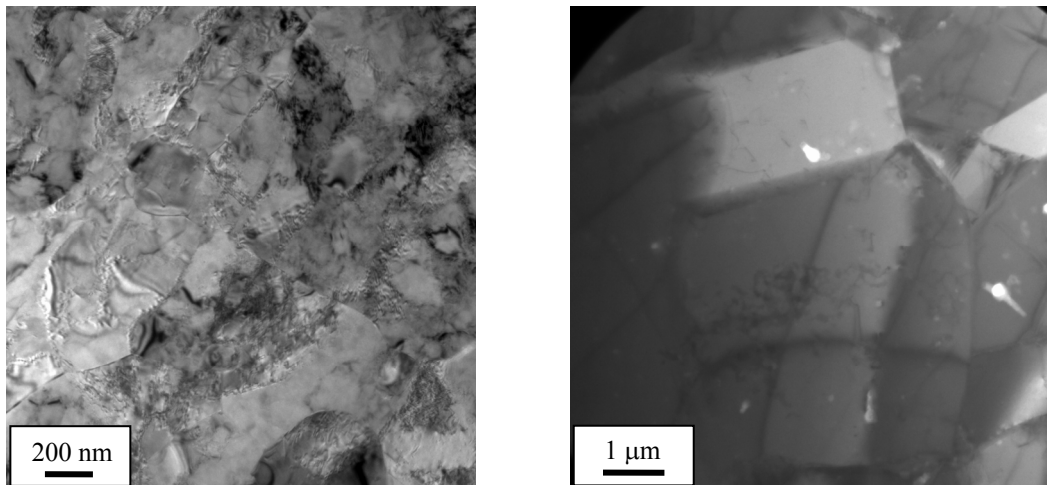


Figure 1: TEM images of nanocrystalline Cu (left) and microcrystalline Cu (right).

nanocrystalline i.e. grain size $< 100\text{nm}$, it is a good representation of materials with grain size approaching the nanocrystalline scale. Tensile strength measurements are conducted for the nanocrystalline and microcrystalline samples, and the results are shown in Fig 2a. The measured yield strength of nanocrystalline Cu is 425 MPa, whereas for microcrystalline sample it is 91 MPa. Also, the high cycle fatigue data of the same material from a previous study [7, 8] is shown in Fig 2b. These results clearly show that the grain refinement has caused a significant increase in the tensile and high cycle fatigue strength of copper. Also, orientation imaging microscopy (OIM) is used to determine the misorientation distribution of the grains in nanocrystalline Cu. The inverse pole figures are shown in Fig 3a, 3b and 3c, and the disorientation angle distribution is shown in Fig 3d. These micrographs show that there is a larger fraction of small angle boundaries ($< 15^\circ$ disorientation) in the nanocrystalline material. Also from these micrographs, it can be observed that there are concentrated regions of small angle boundaries separated by large angle boundaries. These regions of the small angle boundaries are of similar size as that of the grains of microcrystalline Cu that was used as the precursor for the ECAE process. Based on the authors' understanding, the interior of microcrystalline undergoes refinement into smaller grains forming the low angle boundaries and the large angle boundaries represent the original boundaries of the microcrystalline Cu. Similar OIM results are obtained in other regions of the nanocrystalline samples (not shown here), further verifying our analysis.

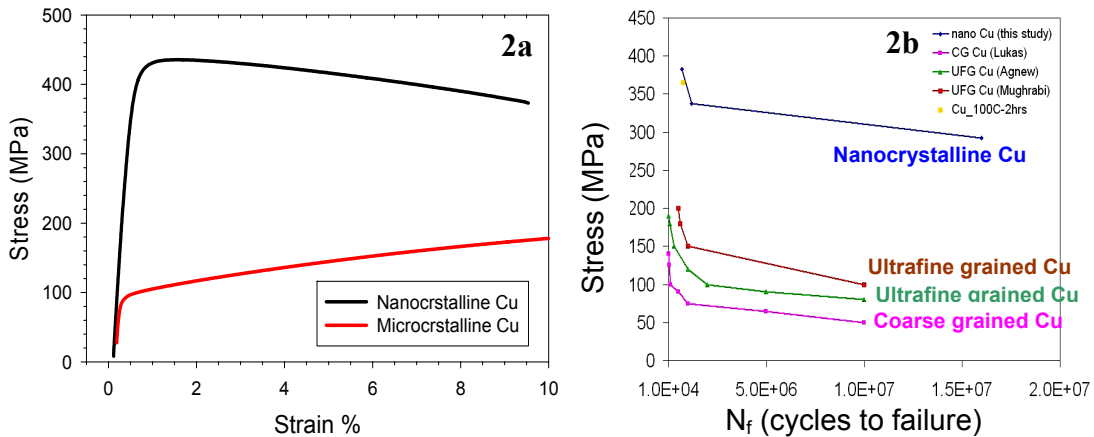


Figure 2: Comparison of tensile strength (Fig. 2a) and high cycle fatigue behavior [7,8] (Fig. 2b) of nanocrystalline and microcrystalline Cu.

3. Experimental Method and Results

The fatigue crack growth tests are conducted as per the ASTM E647 standard using compact type specimens. The outside dimensions ($1.25W$) of the nanocrystalline sample is limited by the size of the ECAE die to 22.86 mm where W is the distance between the center of the loading pin and the back face of the sample. However, larger microcrystalline Cu samples with a width ($1.25W$) of 47.63 mm are prepared to maintain small scale yielding and linear elastic conditions over the entire range of the stress intensity factor (ΔK) values. The

tests are conducted at room temperature under tension-tension loading with loading ratio (R) of 0.1 and the crack length measurements are recorded at increments of 0.2 mm. The crack size is calculated using the compliance method by measuring the crack mouth opening displacement. All samples are fatigue precracked to 1 mm crack length. The precracked samples are tested using the decreasing ΔK method with a normalized K-gradient of -0.08 mm^{-1} . The decreasing ΔK method maintains a stable crack face at longer crack lengths, thereby obtaining maximum data for each test sample. After the completion of the tests, crack length corrections are applied by visually measuring the precrack and final crack sizes from the fracture surface to account for any differences with

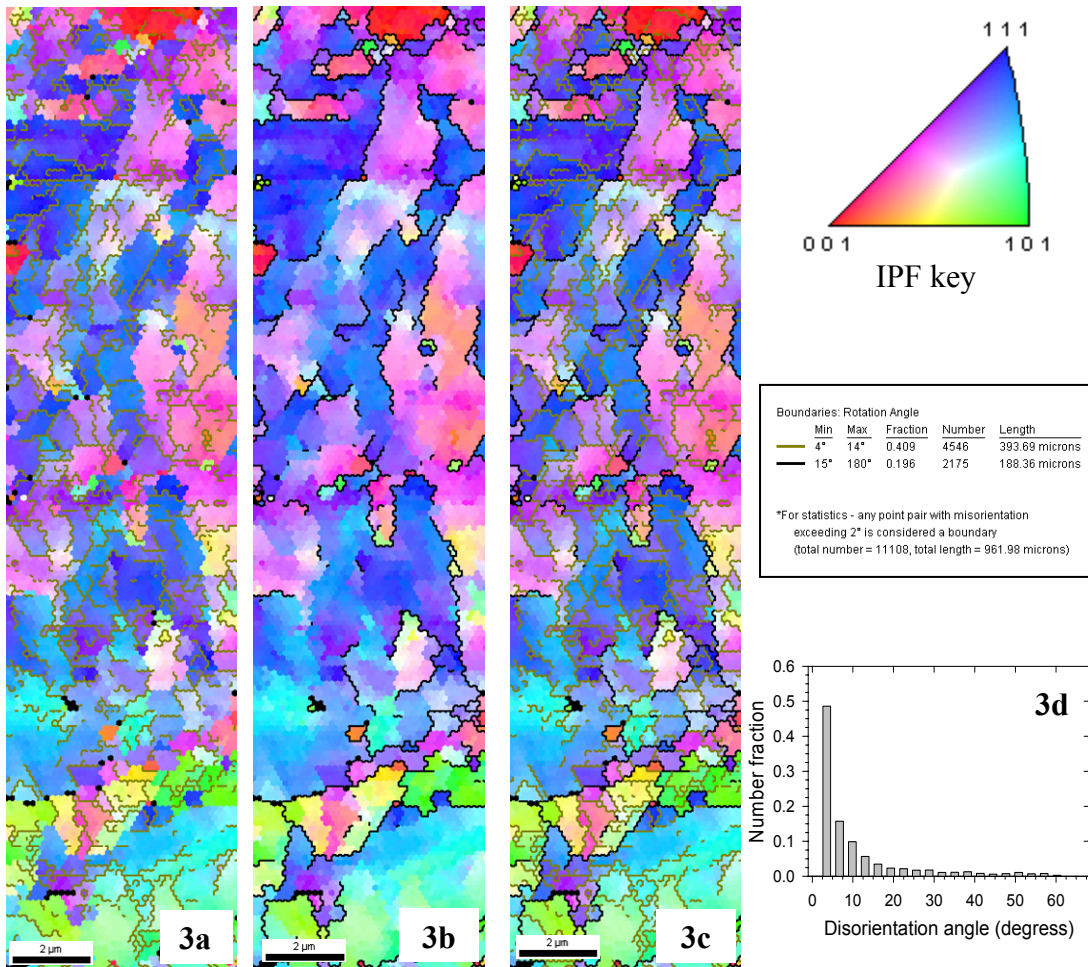


Figure 3: Inverse pole figures (IPF) of nanocrystalline Cu showing the low angle boundaries, colored green (Fig. 3a), high angle boundaries, colored black (Fig. 3b), and the low and high angle boundaries in the same figure (Fig. 3c). The grains are colored by their orientation of their normal to the surface, corresponding to the IPF key. The grain misorientation distribution function is shown in Fig. 3d.

the compliance measurements and for crack tunneling. Due to the smaller size of the nanocrystalline Cu samples, multiple tests are conducted to obtain data for the entire range of ΔK (Figure 4a), whereas only one test of the microcrystalline Cu was needed for the entire ΔK range (Figure 4b). Two fatigue crack growth tests of the microcrystalline Cu are conducted to check for repeatability. The comparison of the fatigue crack growth results for nanocrystalline and microcrystalline Cu is shown in Figure 5.

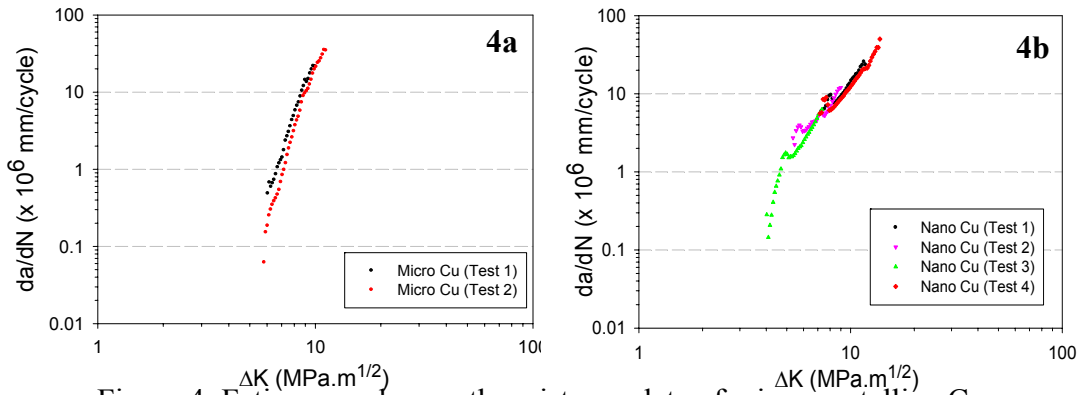


Figure 4: Fatigue crack growth resistance data of microcrystalline Cu (Fig. 4a) and nanocrystalline Cu (Fig. 4b)

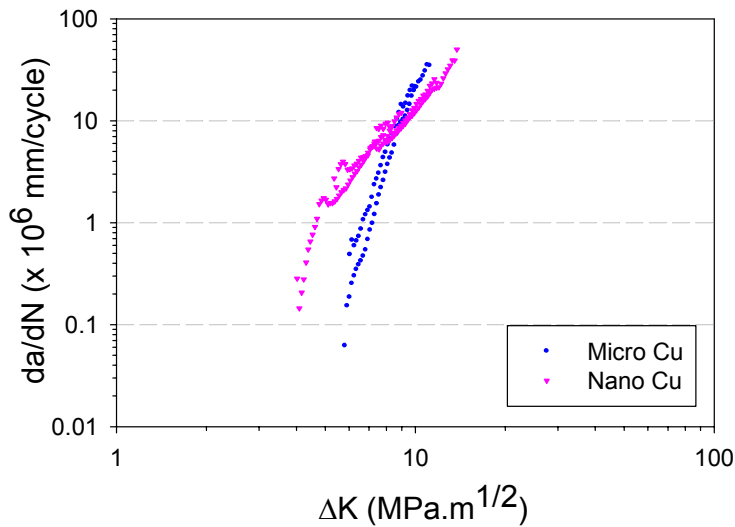


Figure 5: Comparison of fatigue crack growth resistance of microcrystalline and nanocrystalline Cu.

4. Analysis and Discussion

The results in Fig. 5 demonstrate that there is an effect of grain size on the fatigue crack resistance of Cu, and the plots show a distinct crossover. Nanocrystalline Cu has a greater resistance at higher ΔK values in the Paris regime, but a much lower threshold ΔK compared to microcrystalline Cu. The optical micrographs of the fracture surfaces are shown in Fig 6. Formation of a dark band is observed

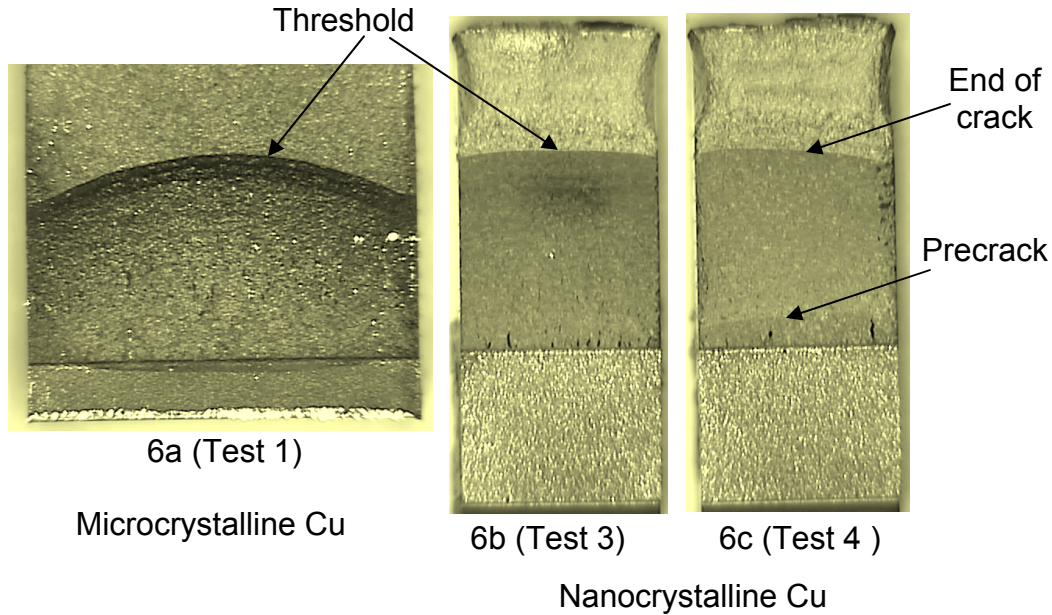


Figure 6: Optical micrographs of fracture surface of microcrystalline Cu (left) and nanocrystalline Cu (middle and right).

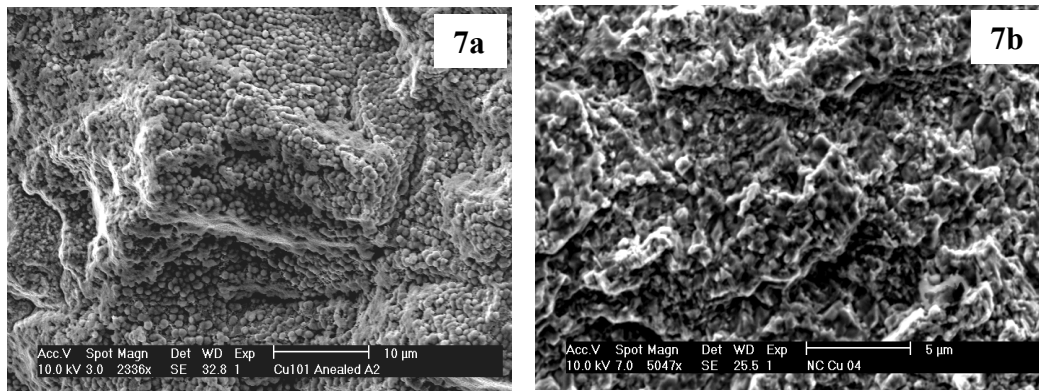


Figure 7: SEM image fracture surface near threshold region of microcrystalline Cu (Fig. 7a) and nanocrystalline Cu (Fig. 7b)

near the threshold area of the microcrystalline Cu sample (Fig. 6a), but is absent in nanocrystalline sample (Fig. 6b).

The SEM and EDS analysis of the threshold region showed the presence of round particles of copper oxide (Cu-82.66 wt.%, O-17.34 wt.%) only in the microcrystalline sample, see Fig. 7. Since the loading ratio is quite low ($R = 0.1$), these oxide particles can cause crack closure effect resulting in lower ΔK_{eff} near the threshold region. A lower ΔK_{eff} will result in a higher fatigue crack growth resistance which could explain the higher threshold value for the microcrystalline Cu sample. The crack closure effect due to the oxide particles can be verified by conducting fatigue crack growth tests at higher loading ratios. At higher loading

ratios it is expected that the crack closure effect will be very minimal and nanocrystalline and microcrystalline Cu will have similar ΔK threshold values.

To analyze the effect of fatigue cyclic loading on the microstructure, Vickers microhardness (HV) measurements are conducted systematically in the plastic zone of the crack tip and at various distances normal to the crack, see Fig. 8a. The microhardness results for two sets of indents for each material is shown in Fig. 8b and their measurement location between each set of indents is 1.0 mm. From these microhardness results it can be seen that there is an increase in hardness in the plastic zone of microcrystalline Cu (near the crack surface), whereas there is considerable softening for nanocrystalline Cu. Also, comparing the two sets of data for each sample in Fig. 8b, it seems that the degree of softening and hardening near the crack surface is greater at higher ΔK levels. Although, this phenomenon needs to be verified with more data before any final conclusion can be drawn.

The increase in microhardness in the plastic zone of microcrystalline Cu is expected due to work hardening. However, the only explanation for the softening in the plastic zone for nanocrystalline Cu is due to stress driven recovery and possibly grain coalescence. Stress driven grain coarsening has been observed previously in nanocrystalline materials using experiments and simulations. Zhang et al. [10] conducted microhardness measurements at $-190\text{ }^\circ\text{C}$ for nanocrystalline Cu and observed grain growth in the vicinity of indent. Due to the large fraction of low angle grain boundaries in these samples, the grain growth mechanism was attributed to stress driven grain rotation and grain coalescence. Also, molecular dynamics simulations by Schiotz [11] for cyclic loading ($R = -1$) of

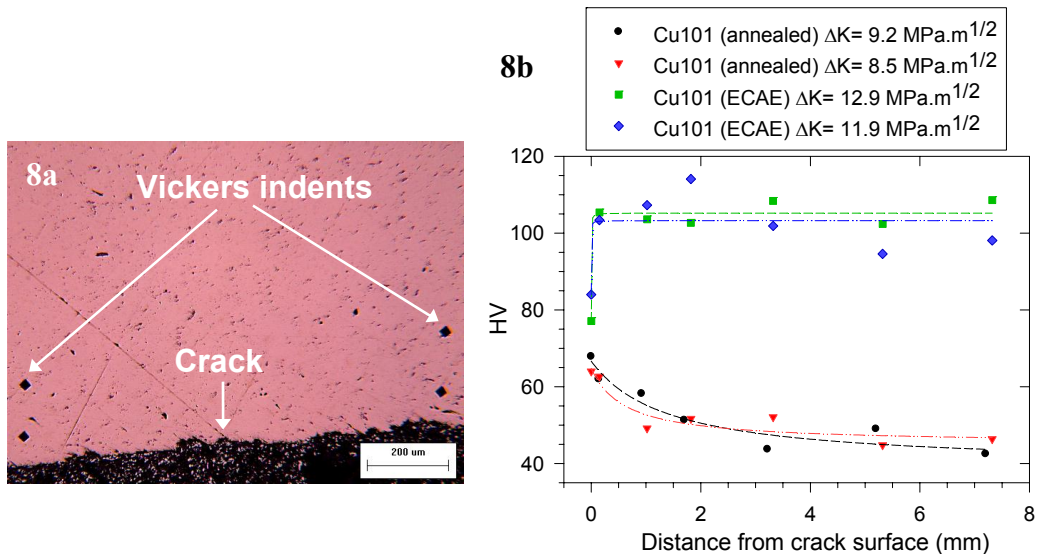


Figure 8: Optical micrograph of fractured specimen showing position of microhardness measurements, using load 0.025 kg (Fig 8a). Microhardness results for microcrystalline and nanocrystalline Cu (Fig 8b). Also, the estimated ΔK at the location of measurement is given in the legend.

nanocrystalline copper with grain size of 10 and 15 nm, showed grain rotation and grain coalescence as the major mechanisms of deformation. Due to the smaller size of grains in the nanocrystalline sample, dislocation mechanisms inside the grains are suppressed and grain boundary mediated processes such as diffusion and sliding became more dominant resulting in grain rotation and grain coalescence [11]. Also, creep deformation tests of nanocrystalline Cu at ambient temperature and a stress level of 87 percent of the yield strength exhibited measurable strain at both primary and steady-state stages [7, 8]. Similar creep behavior is observed in microcrystalline Cu, but only above 35 percent of its melting temperature in Kelvin. This clearly indicates that the high diffusivity of atoms at finer grain sizes that can cause changes in the microstructure of nanocrystalline Cu under the influence of stress at ambient temperature. It is observed from the TEM images (Fig. 1) that the dislocation density in the material processed by severe plastic deformation (ECAE) is quite high. Since the grain size of the material in this study is much higher (350 nm), stress driven grain growth may not explicitly occur in this material. However, recovery by movement and annihilation of dislocations under cyclic stress cannot be ruled out. The dominance of low angle boundaries (Fig. 3) can also cause softening/coarsening by simply rearranging these low energy boundaries, perhaps with little need for grain boundary sliding or grain rotation.

The recovery in the plastic zone of the nanocrystalline sample can explain the increased fatigue crack growth resistance at the higher ΔK levels seen in Fig. 5. In the nanocrystalline samples, the grains in the plastic zone are able to absorb the deformation energy to recover and rotate thus imparting a greater fatigue resistance. These mechanisms are not available in the microcrystalline Cu sample due the lower volume fraction of grain boundaries. To further understand the effect of stress on the microstructure, microhardness measurements are conducted in the plastic zone at various stress intensity levels and the results are shown in Fig. 9a. Based on these results it can be seen that there is a drop in the hardness value at a stress level of about $9 \text{ MPa}\cdot\text{m}^{1/2}$, indicating that a critical stress level is required for stress driven recovery to occur. It is also well understood that grain growth in nanocrystalline materials can occur under the influence of stress and/or temperature [6, 10, 12, 13]. To compare the extent of recovery from these two mechanisms, microhardness measurements of the nanocrystalline material annealed at various temperatures from 250 °C to 700 °C is obtained and compared with the stress driven grain growth results, shown in Fig. 9b. From this figure it can be seen that the nanocrystalline material fully recrystallizes at 250 °C, and any increase in annealing temperature does not cause any change in the microhardness. Comparing the effect of stress and temperature on the microstructural stability (Fig 9b), the stress driven mechanisms may not have caused full recrystallization due the difference in the microhardness measurements after the recovery mechanisms have occurred. If the material is placed in operation at elevated temperatures ($>100 \text{ }^\circ\text{C}$), for example in microelectronics, it is expected that the extent of grain growth in the plastic zone

of nanocrystalline Cu will be much greater and will also affect the fatigue crack growth performance.

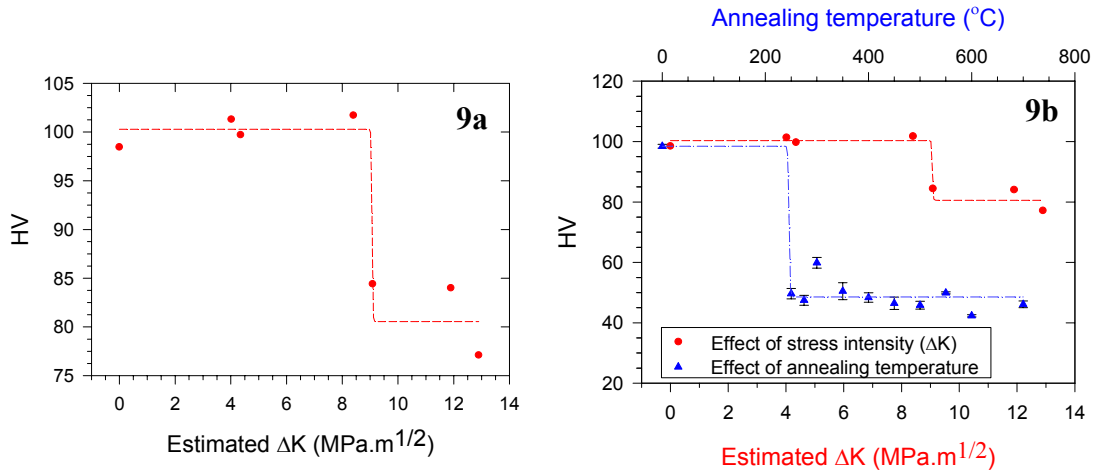


Figure 9: Effect of stress intensity in the plastic zone near the crack on the microhardness for nanocrystalline Cu (Fig 9a). Comparison of stress and temperature driven grain growth for nanocrystalline Cu (Fig 9b). The values for effect of annealing temperature represent average of three measurements.

Conclusions

It has been previously shown that nanocrystalline Cu has improved mechanical strength and high cycle fatigue resistance compared to its microcrystalline counterpart. In this work, comparison of fatigue crack growth behavior at room temperature of nanocrystalline Cu and microcrystalline Cu is presented, using compact specimens in compliance with the ASTM method. The results show a cross-over in the fatigue crack growth response. Due to the softening of the material near the crack tip, stress driven recovery in the nanocrystalline Cu are shown to be the major mechanisms for the increased fatigue crack growth resistance. In the future work, grain size measurements using TEM will be conducted in the plastic zone to check for changes in the grain size and stress driven grain growth. The formation of oxides on the fracture surface in the threshold region of microcrystalline Cu could cause crack closure, ultimately increasing the fatigue resistance near the threshold region.

5. Acknowledgements

The authors would like to thank Dr. K.Ted Hartwig at Texas A&M University, College Station for providing the Cu material and processing it using the ECAE process. The authors would also like to thank Dr. Karen More and Dr. Ed Kenik of the SHaRE user program at the Oak Ridge National Laboratory for their assistance in conducting the TEM and OIM analysis. Funding for this work is in part provided by the Irma and Raymond Giffels' Endowed Chair in Engineering at the University of Arkansas, Fayetteville.

6. References

- [1] Weertman JR. Hall-Petch strengthening in nanocrystalline metals. *Materials Science and Engineering A* 1993;166(1-2):161-167.
- [2] Chokshi AH, Rosen A, Karch J, Gleiter H. On the validity of the Hall-Petch relationship in nanocrystalline materials. *Scripta Metallurgica* 1989;23(10):1679-1684.
- [3] Gleiter H. Nanostructured materials: basic concepts and microstructure. *Acta Materialia* 2000;48(1):1-29.
- [4] Dao M, Lu L, Asaro RJ, De Hosson JTM, Ma E. Toward a quantitative understanding of mechanical behavior of nanocrystalline metals. *Acta Materialia* 2007;55(12):4041-4065.
- [5] Van Swygenhoven H. Grain boundaries and dislocations. *Science* 2002;296(5565):66-67.
- [6] Rajgarhia RK, Koh SW, Spearot D, Saxena A. Microstructure stability of nanocrystalline materials using dopants. *Molecular Simulation* 2008;34(1):35-40.
- [7] Bansal S. Characterization of Nanostructured Metals and Metal Nanowires for Chip-To-Package Interconnections. In: *Materials Science and Engineering*, Vol. Ph.D. Atlanta: Georgia Institute of Technology, 2006.
- [8] Saxena A, Rajgarhia RK, Bansal S. Design of nanocrystalline materials for structural applications. 2nd Integration and Commercialization of Micro & Nanosystems, MicroNano 2008 Clear Water Bay, Kowloon, Hong Kong, 2008, pp. 1-5.
- [9] Furukawa M, Horita Z, Nemoto M, Langdon TG. Processing of metals by equal-channel angular pressing. *Journal of Materials Science* 2001;36(12):2835-2843.
- [10] Zhang K, Weertman JR, Eastman JA. Rapid stress-driven grain coarsening in nanocrystalline Cu at ambient and cryogenic temperatures. *Applied Physics Letters* 2005;87(6):61921-61921.
- [11] Schiotz J. Strain-induced coarsening in nanocrystalline metals under cyclic deformation. *Materials Science and Engineering A* 2004;375-377(1-2 SPEC ISS):975-979.
- [12] Gai PL, Zhang K, Weertman J. Electron microscopy study of nanocrystalline copper deformed by a microhardness indenter. *Scripta Materialia* 2007;56(1):25-28.
- [13] Gertsman VY, Birringer R. On the room-temperature grain growth in nanocrystalline copper. *Scripta Metallurgica et Materialia* 1994;30(5):577-581.
- [14] Bedorf D, Mayr SG. Grain boundary doping of Cu thin films with Bi: A route to create smooth and stable nanocrystalline surfaces. *Scripta Materialia* 2007;57(9):853-856.